Available online at www.HighTechJournal.org

ISSN: 2723-9535

HighTech and Innovation Journal

Vol. 3, No. 3, September, 2022

Static Elastic Bending Analysis of a Three-Dimensional Clamped Thick Rectangular Plate using Energy Method

F. C. Onyeka [1*], T. E. Okeke [2*], B. O. Mama [2]

[1] *Department of Civil Engineering, Edo State University, Uzairue, Edo State, Nigeria.*

[2] *Department of Civil Engineering, University of Nigeria Nsukka, Nigeria.*

Received 03 June 2021; Revised 16 July 2022; Accepted 02 August 2022; Available online 16 August 2022

Abstract

Analytical formulations and solutions for the thick rectangular plate static analysis with clamped support based on a three-dimensional (3-D) elasticity theory is developed using the energy method. The theoretical model, whose formulation is based on the static elastic principle as already reported in the literature, is presented herein to obviate the shear correction coefficients while considering shear deformation effect and transverse normal strain/stress in the analysis. The equilibrium equations are obtained using 3-D kinematic and constitutive relations. The deflection and rotation functions, which are the solutions of the equilibrium equation, are obtained in closed form using a general variational technique for solving the boundary value problem. The minimization energy equation yields the general equation which was used to obtain the theoretical model for the deflection and stresses of the plate. The results are compared with the available literature and the results-computed trigonometric displacement function shows that this 3-D predicts the vertical displacement and the stresses more accurately than previous studies considered in this paper. The result showed that the percentage difference between the present work and those of 2-D Mindlin FSDT, 2-D numeric analysis, and 2-D HSDT of polynomial shape functions was about 3.02%, 0.62%, and 0.33%, respectively. It is concluded that the 3-D trigonometric model gives an exact solution, unlike other 2-D theories, and can be used for clamped-supported thick plate analysis.

Keywords: Exact Static Theory; Equilibrium Equation; Bending of 3-D Clamped Plate; Trigonometric Model.

1. Introduction

Plates are three-dimensional structural elements with spatial dimensions along x, y, and z axes, whose applications are prevalent in different aspects of engineering, such as marine, naval, aerospace, mechanical, and structural engineering. Plates can be classified in terms of shapes such as: quadrilateral, square, circular, or rectangular. Depending on their constituent materials, they may also be classified as isotropic, anisotropic, orthotropic, homogeneous, or non-homogeneous. They can also be defined based on thickness as thin, thick, or moderately thick plates [1, 2]. As regards to its span-to-depth ratio (a/t), Mahi et al. (2015) [3] and Timoshenko & Woinowsky-Krieger (1959) [4] classified rectangular plates with $50 \leq a/t \leq 100$ as thin plate, $20 \leq a/t \leq 50$ as moderately thick and $a/t \leq 20$ as thick plate [5]. The use of thick plates has greatly increased in structural engineering as a result of its cost benefits and other advantages such as its light weight, high strength and load resistance ability [6, 7].

In general, plate research consists of buckling, deflection, and vibration analysis [8]. The bending of the thick rectangular plate is considered in this paper. Bending is the deformation of the plate at right angles to the plate surface

* Corresponding author: onyeka.festus@edouniversity.edu.ng; edozie.okeke@unn.edu.ng

http://dx.doi.org/10.28991/HIJ-2022-03-03-03

due to the impact of forces and moments [9, 10]. As a result of applied load, a structural member is displaced and stresses are induced. Consequently, the structure tends to bend to withstand the load. The bending features of plates are strongly influenced by their thickness in comparison with their other parameters [10]. To ensure the stability of thick plates for resisting design load, bending analysis is needed so as to determine the displacements, moments, and stresses at various points of the plate [11, 12].

Many researchers have developed and applied several theories to avoid the complexity of analyzing rectangular plates as a three-dimensional element. These theories include the classical plate theory (CPT) and the refined plate theory (RPT). These theories offer solutions to plate problems in either exact or approximate form. Classical plate theory [13] cannot ascertain the proper bending behavior of thick plates as the shear deformation effect is overlooked [14, 15]. The introduction of shear deformation effects on the plate displacements distinguishes thick plate theories from thin plate theories. This resulted in the formulation of refined plate theories. The refined plate theories (RPT), which can be employed for thick plate analysis [16], consists of first-order shear deformation theory (FSDT), also called Reissner-Mindlin theory [17-19], and higher-order shear deformation theories (HSDTs), that provide zero shear stress conditions at the upper and underside of the plates without the shear correction factor [20-22].

Refined plate theories, which has been used by scholars such as [23-25], consider five strains, five stress components, assuming the normal stress and strain along the z-axis to be zero. Refined plate theories are inadequate to express an accurate bending response of a typical 3-D thick plate. In order to overcome the errors of refined plate theories (RPT) in analysis of rectangular plates, three-dimensional theory must be employed to ensure that no stress or strain element is assumed to be zero. For a typical 3-D thick plate analysis, refined plate theories are indelicate, hence the need for precise results through the application of 3-D theory is justified.

The purpose of this research is to apply 3-D theory in solving the problem of deflection for a clamped isotropic rectangular thick plate, investigating the impact of aspect ratio and displacement of the moment, shear force, stresses, and stress resultant of the plate using the Energy method. This study was undertaken with the following objectives in mind:

- To create the internal energy of a three-dimensional rectangular thick plate;
- To generate the compatibility and overall governing equations of the plate and derive equations of displacements and shear deformation slope coefficient for x, y and z coordinates;
- To obtain the exact expressions of the displacements, bending moment, shear force and stresses for the thick rectangular plate.

2. Literature Review

For a rectangular SSSS Kirchhoff plate, the Ritz method was used by Nwoji et al. (2018) [26] to analyze the plate bending problem. The method used by the authors yielded exact identical solutions as the exact results obtained by those who employed the Navier double Fourier sine series method. Using the exact deflection shape function, the authors obtained an exact solution. Ike (2017) [27] applied the Kantorovich-Galerkin method in studying the bending of CSSS plates with an assumed displacement function. The author formulated the equation of equilibrium in line with the work of Euler-Lagrange and solved to obtain the deflection and bending moment coefficients for deflection at the center of the plates under the uniform. The author did not consider the stresses in the direction of thickness axis neither was plates the CCCC boundary condition taken into account. The author did not apply the general variational method in the derivation of the displacement function and shape function used was assumed, which made the result not a close-form solution.

Using an analytical method, Onyeka et al. (2019) [2] employed third-order refined theory for solving the bending of a thick rectangular plate that is simply supported on all the edges. To determine displacement coefficients, the equation of total stored energy of a thick plate that was generated from elastic. Integral direct integration method of the exact analytical solution approach was used to determine the work, stresses, displacement and the shear deformation equation and the values obtained from their study conformed to the values from previous studies. However, the authors did not consider a full 3-D analogy for a typical three-dimensional plate with all round clamped edges using the energy method.

Ibearugbulem et al. (2018) [28] applied shear deformation theory with a polynomial shape function to analyze the bending of CCCC rectangular thick plates. As with other higher-order theories, the condition of zero shear stress on the surfaces of the plate were met with the transverse shear stress derived from the constitutive relation of the theory. The authors did not consider a trigonometric shape function. Even though the result of their displacements and stresses, a 3-D theory was not applied. Onyeka & Edozie (2021) [29] analyzed the displacements and stresses of thick rectangular CCFC plate applying the higher order polynomial which was derived from the governing equation using the general variation method. The results of their study agreed well with those of refined plate theory, but varied more with the value of the classical plate theory. The considerations of authors will not yield a good result for a 3-D plate because it is limited to a 2-D plate theory. The trigonometric shape function and CCCC boundary condition was not considered.

Analyzing the problem of displacement-stresses in thick plates with simply supported edges, Sayyad & Ghugal, (2012) [23] used the refined theory of shear deformation and exponential functions. The shear transverse distortion and rotary inertia were found using the theory and the functions in thickness coordinate form. Compared with other refined plate theories, the displacements and stresses achieved in their result were satisfactory. The authors did not consider trigonometric displacement function in an energy method using the 3-D theory. Also, their analysis did not cover for thick plates with all-round clamped boundary conditions. Onyeka et al. (2020) [30] analyzed the bending behavior of rectangular thick CSCS and SCFS plates based on fourth-order polynomial shear deformation function. The authors developed a new approach to achieve the critical load of the plate from the established equation. The deflection and stresses obtained in their study were identical with the other order theories, but they did not analyze the in-plane displacement and moment that induce mending in the plate. Also, the author neither analyzes the plate as a typical 3-D element nor did they consider a thick plate of all round clamped edges.

Applying the numerical method on account of the three-dimensional theory of elasticity, the study of bending solutions of thick plates with clamped edge conditions, was carried out Grigorenko et al. (2013) [31]. The authors employed two coordinate directions of spline collocation and the resultant displacements and stresses in the clamped thick rectangular plates were satisfactory. The result of their study were not exactly because they did not consider the analytical approach neither did they use the energy method that is more simplified.

Onyeka & Ibearugbulem (2020) [32], used the direct variation energy method to obtain closed form solutions for bending analysis of CCCC and CCFC thick rectangular plates, applying the nonlinear strain-displacement polynomial shape function of fourth order shear deformation theory. From the principle of variational calculus, the authors obtained the governing equations which were used to solve the deflection problem of the plates. They also developed formulas for calculating actual and maximum lateral loads imposed on the plate before deformation gets to the specified maximum specified limit and elastic yield respectively. Their result confirmed that the actual load that causes the bending problem can be predicted using this theory. The 3-D theory was also not employed, nor did the authors consider the use of the trigonometric shape function. The authors investigated only the aspect ratio effects on the critical thickness of the plate without considering the displacement and stresses. A three-dimensional analysis of a thick SSSS plate was presented analytically by Fu et al. (2022) [33].

To obtain a total potential energy function, strain and stress with six components each, were used by the shear deformation theory of third order. The rotation and deflection expressions were derived from the solutions of compatibility equations that were obtained by minimizing the function with respect to shear deformation rotations. The deflection equation was found by solving the governing equation derived from further minimization of the function with respect to deflect. The values of the calculated deflections and stresses obtained from the 3-D analysis were coarse compared with those of refined plate theories. The work is limited as there is no application of trigonometric displacement functions which produces an exact solution.

Ibearugbulem & Onyeka (2020) [34] employed a direct variation energy method to solve the bending problem of clamped rectangular plates using third order plate theory. The method used did not require shearing correction factors and the results obtained revealed its precision by numerical comparison. The authors did not analyze for the critical lateral load and the solutions of their study were not exactly as a result of the assumed shape function and non-application of the general variational method. The authors did not consider the use of trigonometric displacement function and did not apply the 3D theory. Most of these reviewed studies are mostly based on refined plate theories. Aside from the work by Ibearugbulem & Onyeka et al. (2020) [34], one can hardly see work on the bending behavior of thick plates based on 3-D theory. The need for this current research work cannot be neglected, as it is worthwhile to fill this gap in the literature. The peculiarity of this study with the various previous respective works resides in the type of plate theory, method of analysis, the displacement functions, and the plate supports. In this study, the general variation of the total potential energy was performed in order to get an exact trigonometric shape function from the elastic principle without assumption. Investigating the bending features for a CCCC rectangular, this work also went ahead to determine the displacements and stresses of the plate using 3-D plate theory.

3. Methodology

The research methodology of this study is presented by considering a rectangular plate in Figure 1 as a three-dimensional element in which the deformation exists in the three axis: length (a), width (b) and thickness (t). The analytical approach of the energy method was used to obtain formulas for the analysis.

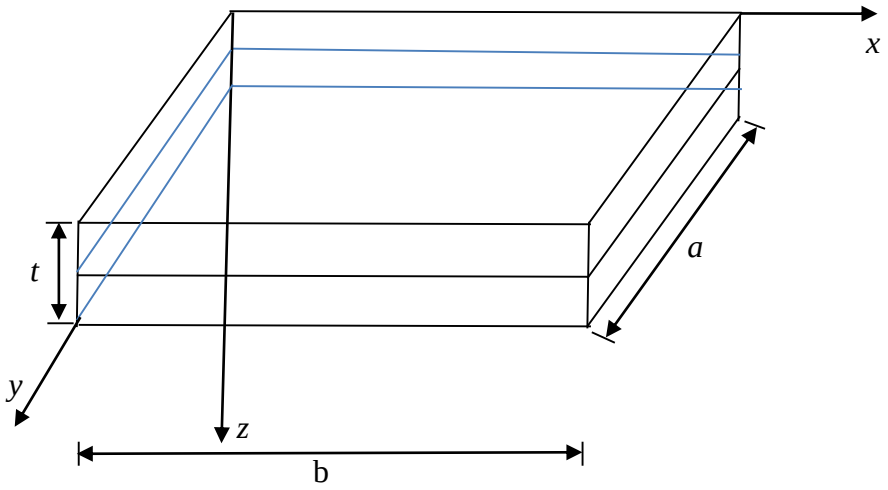

Figure 1. An element of thick rectangular plate showing middle surface

Figure 2 is a flowchart which indicates the procedures of formulating the potential energy equation in the form of the kinematics and three-dimensional constitutive relations for a static elastic theory of plate, thereafter, the governing equations were derived and solved to obtain formula for the analysis.

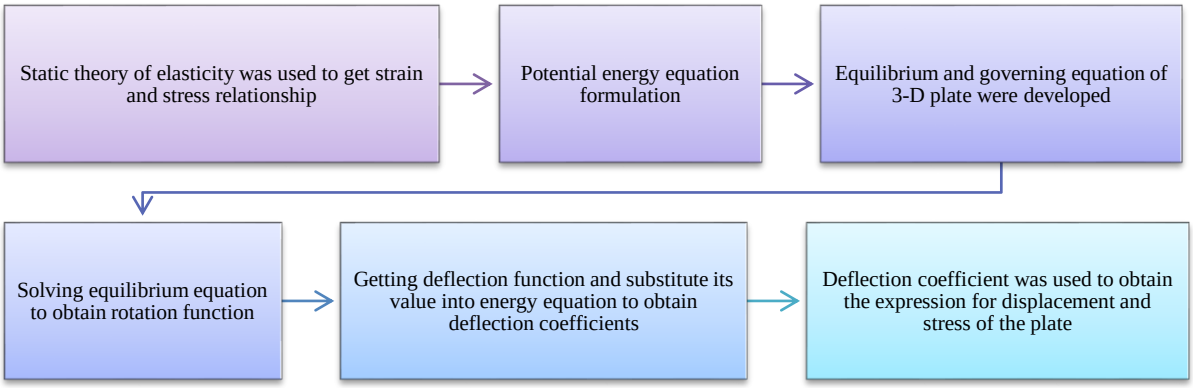

Figure 2. Flowchart to the article analysis procedure as presented in the research methodology

3.1. Kinematics

The 3-D displacement kinematics along x, y and z axis (u, v and w) shown in the Figure 3 are obtained assuming that the x-z section and y-z section, is no longer normal to x-y plane after bending.

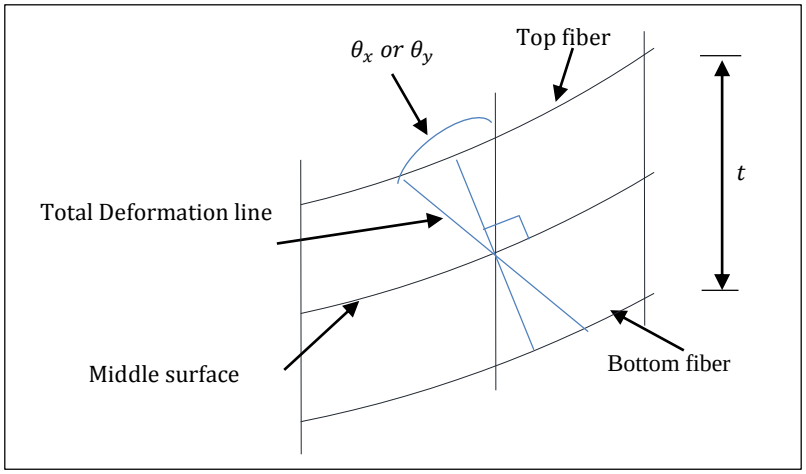

Figure 3. Rotation of x-z (or y-z) section after bending

Resolving the deformation diagram in Figure 3 using trigonometric relations, the algebraic relationship between the displacement and slope along the x axis and y becomes:

$$\theta_x = \frac{\partial u}{\partial z} \tag{1}$$

$$\theta_y = \frac{\partial v}{\partial z} \tag{2}$$

where, θ_x and θ_y is the shear deformation rotation along x axis and y axis.

Taking into account, the thick plate assumption as stated in this section, the non-dimensional form of the Equations 1 and 2 gives:

$$\theta_x = \frac{1}{\mathrm{t}}.\frac{\partial u}{\partial s} \tag{3}$$

$$\theta_y = \frac{1}{\mathrm{t}}.\frac{\partial v}{\partial s} \tag{4}$$

Where:

$$z = ts \tag{5}$$

Re-arranging Equation 3 and 4 gives:

$$u = ts.\theta_{sx} \tag{6}$$

$$v = ts.\theta_{sy} \tag{7}$$

where, u and v is the in-plane displacement along x-axis and y axis respectively, thus, the six non-dimensional coordinates strain components were derived using strain-displacement expression according to Hooke's law and presented in Equations 8 to 13:

$$\varepsilon_x = \frac{1}{\mathrm{a}}.\frac{\partial u}{\partial R} \tag{8}$$

$$\varepsilon_y = \frac{1}{\mathrm{a}\beta}.\frac{\partial v}{\partial Q} \tag{9}$$

$$\varepsilon_z = \frac{1}{\mathrm{t}}.\frac{\partial w}{\partial s} \tag{10}$$

$$\gamma_{xy} = \frac{1}{\mathrm{a}\beta}.\frac{\partial u}{\partial Q} + \frac{1}{\mathrm{a}}.\frac{\partial v}{\partial R} \tag{11}$$

$$\gamma_{xz} = \frac{1}{\mathrm{t}}.\frac{\partial u}{\partial s} + \frac{1}{\mathrm{a}}.\frac{\partial w}{\partial R} \tag{12}$$

$$\gamma_{yz} = \frac{1}{\mathrm{t}}.\frac{\partial v}{\partial s} + \frac{1}{\mathrm{a}\beta}.\frac{\partial w}{\partial Q} \tag{13}$$

where, $\varepsilon_x, \varepsilon_v$ and ε_z are normal strain along x axis, y axis and z axis respectively, $\gamma_{xv}, \gamma_{xz}\ and\ \gamma_{vz}$ represents the shear strain in the plane parallel to the x-y, x-z and y-z plane.

3.2. Constitutive Relations

The three dimensional constitutive relation is determined using a generalized Hooke's principle as:

$$\begin{bmatrix}\sigma_x\\ \sigma_y\\ \sigma_z\\ \tau_{xz}\\ \tau_{yz}\\ \tau_{xy}\end{bmatrix} = \frac{\mathrm{E}}{(1+\mu)(1-2\mu)}\begin{bmatrix}(1-\mu) & \mu & \mu & 0 & 0 & 0\\ \mu & (1-\mu) & \mu & 0 & 0 & 0\\ \mu & \mu & (1-\mu) & 0 & 0 & 0\\ 0 & 0 & 0 & \left(\frac{1-2\mu}{2}\right) & 0 & 0\\ 0 & 0 & 0 & 0 & \left(\frac{1-2\mu}{2}\right) & 0\\ 0 & 0 & 0 & 0 & 0 & \left(\frac{1-2\mu}{2}\right)\end{bmatrix}\begin{bmatrix}\varepsilon_x\\ \varepsilon_y\\ \varepsilon_z\\ \gamma_{xz}\\ \gamma_{yz}\\ \gamma_{xy}\end{bmatrix} \tag{14}$$

where, E and μ are the modulus of elasticity and Poisson's ratio.

The six stress components were obtained by substituting Equations 8 to 13 into Equation 14 and simplifying the outcome as:

$$\sigma_x = \frac{\mathrm{E}}{(1+\mu)(1-2\mu)}\left[(1-\mu)\frac{\mathrm{ts}}{\mathrm{a}}.\frac{\partial\theta_{sx}}{\partial R} + \mu\frac{\mathrm{ts}}{\mathrm{a}\beta}.\frac{\partial\theta_{sy}}{\partial Q} + \mu\frac{1}{\mathrm{t}}.\frac{\partial \mathrm{w}}{\partial S}\right] \tag{15}$$

$$\sigma_y = \frac{\mathrm{E}}{(1+\mu)(1-2\mu)}\left[\mu\,\mathrm{ts}.\frac{\partial\theta_x}{a\partial R} + \frac{(1-\mu)\mathrm{ts}}{a\beta}.\frac{\partial\theta_y}{\partial Q} + \frac{\mu}{t}.\frac{\partial w}{\partial S}\right] \tag{16}$$

$$\sigma_z = \frac{\mathrm{E}}{(1+\mu)(1-2\mu)}\left[\mu\,\mathrm{ts}.\frac{\partial\theta_x}{a\partial R} + \frac{\mu\mathrm{ts}}{a\beta}.\frac{\partial\theta_y}{\partial Q} + \frac{(1-\mu)}{t}.\frac{\partial w}{\partial S}\right] \tag{17}$$

$$\tau_{xy} = \frac{E(1-2\mu)}{(1+\mu)(1-2\mu)} \cdot \left[\frac{\text{ts}}{2a\beta}\frac{\partial \theta_x}{\partial Q} + \frac{\text{ts}\partial \theta_y}{2a\partial R}\right] \quad (18)$$

$$\tau_{xz} = \frac{(1-2\mu)E}{(1+\mu)(1-2\mu)} \cdot \left[\frac{\theta_x}{2} + \frac{1}{2a}\frac{\partial w}{\partial R}\right] \quad (19)$$

$$\tau_{yz} = \frac{(1-2\mu)E}{(1+\mu)(1-2\mu)} \cdot \left[\frac{\theta_y}{2} + \frac{1}{2a\beta}\frac{\partial w}{\partial Q}\right] \quad (20)$$

3.3. Strain Energy

The strain energy (U) is mathematically defined as:

$$U = \frac{abt}{2}\int_0^1 \int_0^1 \int_{-0.5}^{0.5} \left(\sigma_x \varepsilon_x + \sigma_y \varepsilon_y + \sigma_z \varepsilon_z + \tau_{xy}\gamma_{xy} + \tau_{xz}\gamma_{xz} + \tau_{yz}\gamma_{yz}\right) dR\, dQ\, dS \quad (21)$$

Substituting the values of stresses (Equations 8 to 13) and strain (Equations 15 to 20) into Equation 21, and integrate the dot product with respect to gives:

$$\begin{aligned} \text{U} = {} & \frac{\text{Et}^3 ab}{24(1+\mu)(1-2\mu)\text{a}^2}\int_0^1 \int_0^1 \left[(1-\mu)\left(\frac{\partial \theta_{sx}}{\partial R}\right)^2 + \frac{1}{\beta}\frac{\partial \theta_{sx}}{\partial R}\cdot\frac{\partial \theta_{sy}}{\partial Q} + \frac{(1-\mu)}{\beta^2}\left(\frac{\partial \theta_{sy}}{\partial Q}\right)^2 + \frac{(1-2\mu)}{2\beta^2}\left(\frac{\partial \theta_{sx}}{\partial Q}\right)^2 + \frac{(1-2\mu)}{2}\left(\frac{\partial \theta_{sy}}{\partial R}\right)^2 + \right. \\ & \frac{12.(1-2\mu)}{2\text{t}^2}\left(\text{a}^2{\theta_{sx}}^2 + \text{a}^2{\theta_{sy}}^2 + \left(\frac{\partial \text{w}}{\partial R}\right)^2 + \frac{1}{\beta^2}\left(\frac{\partial \text{w}}{\partial Q}\right)^2 + 2\text{a}.\theta_{sx}\frac{\partial \text{w}}{\partial R} + \frac{2\text{a}.\theta_{sy}}{\beta}\frac{\partial \text{w}}{\partial Q}\right) + 0 * 2\frac{\mu\text{a}}{\text{t}^2}.\left(\frac{\partial \theta_{sx}}{\partial R}.\frac{\partial \text{w}}{\partial S} + \right. \\ & \left.\left. \frac{1}{\beta}.\frac{\partial \theta_{sy}}{\partial Q}.\frac{\partial \text{w}}{\partial S}\right) + \frac{(1-\mu)\text{a}^2}{t^4}\left(\frac{\partial \text{w}}{\partial S}\right)^2\right] \text{dR dQ} \end{aligned} \quad (22)$$

Where;

$$D^* = \frac{Et^3}{12(1+\mu)(1-2\mu)} \quad (23)$$

3.4. Energy Equation Formulation

The total potential energy is mathematically expressed as:

$$\prod = \text{U} - \text{V} \quad (24)$$

$$V = abqA_1\int_0^1 \int_0^1 h\, dR\, dQ \quad (25)$$

where, V, q, A_1 and h are the external work, uniformly distributed load, coefficient of deflection and shape function of the plate respectively, a and b is the length and breadth of the plate.

Substituting Equations 22 and 25 into Equation 24 gives:

$$\begin{aligned} \Pi = {} & \frac{D^* ab}{2a^2}\int_0^1 \int_0^1 \left[(1-\mu)\left(\frac{\partial \theta_{sx}}{\partial R}\right)^2 + \frac{1}{\beta}\frac{\partial \theta_{sx}}{\partial R}\cdot\frac{\partial \theta_{sy}}{\partial Q} + \frac{(1-\mu)}{\beta^2}\left(\frac{\partial \theta_{sy}}{\partial Q}\right)^2 + \frac{(1-2\mu)}{2\beta^2}\left(\frac{\partial \theta_{sx}}{\partial Q}\right)^2 + \frac{(1-2\mu)}{2}\left(\frac{\partial \theta_{sy}}{\partial R}\right)^2 + \right. \\ & \left. \frac{6(1-2\mu)}{t^2}\left(a^2{\theta_{sx}}^2 + a^2{\theta_{sy}}^2 + \left(\frac{\partial w}{\partial R}\right)^2 + \frac{1}{\beta^2}\left(\frac{\partial w}{\partial Q}\right)^2 + 2a.\theta_{sx}\frac{\partial w}{\partial R} + \frac{2a.\theta_{sy}}{\beta}\frac{\partial w}{\partial Q}\right) + \frac{(1-\mu)a^2}{t^4}\left(\frac{\partial w}{\partial S}\right)^2\right] dR\, dQ - \\ & \int_0^1 \int_0^1 abqhA_1 \partial R \partial Q \end{aligned} \quad (26)$$

3.5. Governing Equation

The solution of the governing equation is presented as the result of energy functional minimization with respect to deflection to give exact plate's shape function:

$$h = [1 \quad R \quad Cos(c_1R) \quad Sin(c_1R)]\begin{bmatrix}a_0\\a_1\\a_2\\a_3\end{bmatrix}.[1 \quad Q \quad Cos(c_1Q) \quad Sin(c_1Q)]\begin{bmatrix}b_0\\b_1\\b_2\\b_3\end{bmatrix}/A_1 \quad (27)$$

$$\theta_x = \frac{c}{a}.\Delta_0.[1 \quad c_1Sin(c_1R) \quad c_1Cos(c_1R)]\begin{bmatrix}a_1\\a_2\\a_3\end{bmatrix}.[1 \quad Q \quad Cos\,(c_1Q) \quad Sin\,(c_1Q)]\begin{bmatrix}b_0\\b_1\\b_2\\b_3\end{bmatrix} \quad (28)$$

$$\theta_y = \frac{c}{a\beta}.\Delta_0.[1 \quad R \quad Cos(c_1R) \quad Sin(c_1R)]\begin{bmatrix}a_0\\a_1\\a_2\\a_3\end{bmatrix}.[1 \quad c_1Sin(c_1Q) \quad c_1Cos(c_1Q)]\begin{bmatrix}b_1\\b_2\\b_3\end{bmatrix} \quad (29)$$

Let;

$$w = A_1.h \tag{30}$$

$$\theta_x = \frac{A_2}{a}.\frac{\partial h}{\partial R} \tag{31}$$

$$\theta_y = \frac{A_3}{a\beta}.\frac{\partial h}{\partial Q} \tag{32}$$

where; A_2 and A_3 are the coefficient of shear deformation along x axis and coefficient of shear deformation along y axis respectively.

Substituting Equations 30, 31 and 32 into 26, gives:

$$\Pi = \frac{D^* ab}{2a^4}\left[(1-\mu){A_2}^2 k_x + \frac{1}{\beta^2}\left[A_2.A_3 + \frac{(1-2\mu){A_2}^2}{2} + \frac{(1-2\mu){A_3}^2}{2}\right]k_{xy} + \frac{(1-\mu){A_3}^2}{\beta^4}k_y + 6(1-2\mu)\left(\frac{a}{t}\right)^2\left(\left[{A_2}^2 + {A_1}^2 + 2A_1A_2\right].k_z + \frac{1}{\beta^2}.\left[{A_3}^2 + {A_1}^2 + 2A_1A_3\right].k_{2z}\right) - \frac{2qa^4k_hA_1}{D^*}\right] \tag{33}$$

Where;

$$k_x = \int_0^1\int_0^1\left(\frac{\partial^2 h}{\partial R^2}\right)^2 dRdQ \tag{34}$$

$$k_{xy} = \int_0^1\int_0^1\left(\frac{\partial^2 h}{\partial R\partial Q}\right)^2 dRdQ \tag{35}$$

$$k_y = \int_0^1\int_0^1\left(\frac{\partial^2 h}{\partial Q^2}\right)^2 dRdQ \tag{36}$$

$$k_z = \int_0^1\int_0^1\left(\frac{\partial h}{\partial R}\right)^2 dRdQ \tag{37}$$

$$k_{2z} = \int_0^1\int_0^1\left(\frac{\partial h}{\partial Q}\right)^2 dRdQ \tag{38}$$

$$k_h = \int_0^1\int_0^1 h\,.dRdQ \tag{39}$$

Minimizing Equation 33 with respect to A_2 gives:

$$\frac{\partial \Pi}{\partial A_2} = (1-\mu)A_2k_x + \frac{1}{2\beta^2}[A_3 + A_2(1-2\mu)]k_{xy} + 6(1-2\mu)\left(\frac{a}{t}\right)^2[A_2 + A_1].k_z = 0 \tag{40}$$

Minimizing Equation 33 with respect to A_3 gives:

$$\frac{\partial \Pi}{\partial A_2} = \frac{(1-\mu)A_3}{\beta^4}k_y + \frac{1}{2\beta^2}[A_2 + A_3(1-2\mu)]k_{xy} + \frac{6}{\beta^2}(1-2\mu)\left(\frac{a}{t}\right)^2([A_3 + A_1].k_{2z}) = 0 \tag{41}$$

Rewriting Equations 34 and 35 gives:

$$\left[(1-\mu)k_x + \frac{1}{2\beta^2}(1-2\mu)k_{xy} + 6(1-2\mu)\left(\frac{a}{t}\right)^2 k_z\right]A_2 + \left[\frac{1}{2\beta^2}k_{xy}\right]A_3 = \left[-6(1-2\mu)\left(\frac{a}{t}\right)^2 k_z\right]A_1 \tag{42}$$

$$\left[\frac{1}{2\beta^2}k_{xy}\right]A_2 + \left[\frac{(1-\mu)}{\beta^4}k_y + \frac{1}{2\beta^2}(1-2\mu)k_{xy} + \frac{6}{\beta^2}(1-2\mu)\left(\frac{a}{t}\right)^2 k_{2z}\right]A_3 = \left[-\frac{6}{\beta^2}(1-2\mu)\left(\frac{a}{t}\right)^2 k_Q\right]A_1 \tag{43}$$

Solving Equations 42 and 43 simultaneously gives:

$$A_2 = MA_1 \tag{44}$$

$$A_3 = NA_1 \tag{45}$$

Let:

$$M = \frac{(r_{12}r_{23} - r_{13}r_{22})}{(r_{12}r_{12} - r_{11}r_{22})} \tag{46}$$

$$N = \frac{(r_{12}r_{13} - r_{11}r_{23})}{(r_{12}r_{12} - r_{11}r_{22})} \tag{47}$$

Where;

$$r_{11} = (1-\mu)k_x + \frac{1}{2\beta^2}(1-2\mu)k_{xy} + 6(1-2\mu)\left(\frac{a}{t}\right)^2 k_z \tag{48}$$

$$r_{22} = \frac{(1-\mu)}{\beta^4}k_y + \frac{1}{2\beta^2}(1-2\mu)k_{xy} + \frac{6}{\beta^2}(1-2\mu)\left(\frac{a}{t}\right)^2 k_{2z} \tag{49}$$

$$r_{12} = r_{21} = \frac{1}{2\beta^2} k_{xy};\ r_{13} = -6(1-2\mu)\left(\frac{a}{t}\right)^2 k_z;\ r_{23} = r_{32} = -\frac{6}{\beta^2}(1-2\mu)\left(\frac{a}{t}\right)^2 k_{2z} \quad (50)$$

Minimizing Equation 33 with respect to A_1 gives:

$$\frac{\partial \Pi}{\partial A_1} = \frac{D^* ab}{2a^4}\left[6(1-2\mu)\left(\frac{a}{t}\right)^2 \left([2A_1 + 2A_2].k_z + \frac{1}{\beta^2}.[2A_1 + 2A_3].k_{2z}\right) - \frac{2qa^4 k_h}{D^*}\right] = 0 \quad (51)$$

That is:

$$6(1-2\mu)\left(\frac{a}{t}\right)^2 \left([A_1 + UA_1].k_z + \frac{1}{\beta^2}.[A_1 + VA_1].k_{2z}\right) - \frac{qa^4 k_h}{D^*} = 0 \quad (52)$$

Factorizing Equations 52 and simplifying gives:

$$6(1-2\mu)\left(\frac{a}{t}\right)^2 A_1 \left([1+U].k_z + \frac{1}{\beta^2}.[1+V].k_{2z}\right) = \frac{qa^4 k_h}{D^*} \quad (53)$$

$$TA_1 = \frac{qa^4 k_h}{D^*} \quad (54)$$

$$A_1 = \frac{qa^4}{D^*}\left(\frac{k_h}{T}\right) \quad (55)$$

Where;

$$T = 6(1-2\mu)\left(\frac{a}{t}\right)^2 * \left([1+U].k_z + \frac{1}{\beta^2}.[1+V].k_{2z}\right) \quad (56)$$

3.6. Numerical Analysis

The numerical analysis of a rectangular thick plate whose Poisson's ratio is 0.3 under CCCC boundary conditions as shown in the Figure 4 and carrying uniformly distributed load (including self-weight) is presented. An exact trigonometric functions as was obtained in the Equation 27 and applied here to get the actual values of the shape functions, coefficients of deflection and shear deformation rotations at x and y axis of the plate.

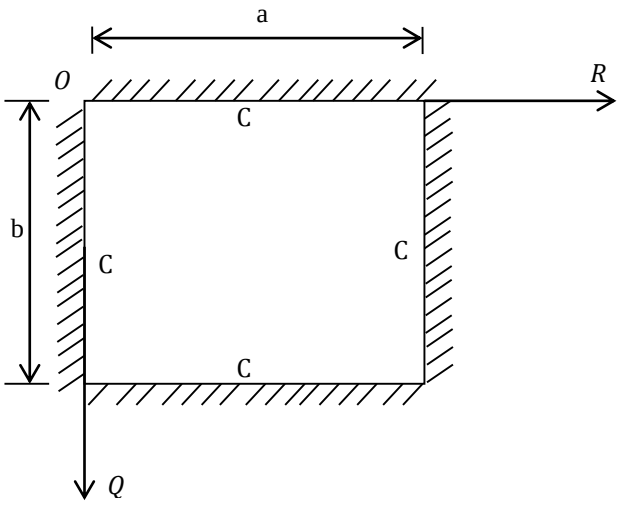

Figure 4. CCCC Rectangular Plate

The boundary conditions of the plate in Figure 4 are as follows:

$$\text{At } R = Q = 0;\ w = 0 \quad (57)$$

$$\text{At } R = Q = 0;\ \frac{dw}{dR} = \frac{dw}{dQ} = 0 \quad (58)$$

$$\text{At } R = Q = 1;\ w = 0 \quad (59)$$

$$\text{At } R = Q = 1;\ \frac{dw}{dR} = \frac{dw}{dQ} = 0 \quad (60)$$

The derived trigonometric deflection $w\,(x, y)$ functions is subjected to a CCCC boundary condition to get the particular solution of the deflection. Hence, the analytical solution of the deflection of the plate in trigonometric form after satisfying the boundary conditions for all edges clamped rectangular plate presented in the Equation 61:

$$w = a_2 \times b_2(\,Cos2\pi R - 1).(Cos2\pi Q - 1) \tag{61}$$

where the coefficient of the deflection,

$$A_1 = a_2 \times b_2 \tag{62}$$

while the shape function

$$h = (\,Cos2\pi R - 1).(Cos2\pi Q - 1) \tag{63}$$

3.7. Exact Displacement and Stress Expression

By substituting the value of A_1, A_2 and A_3 in Equations 49, 38 and 39 into Equation 15 to 20 and substitute appropriately, the in-plane displacement along x-axis becomes:

$$u = ts.\frac{M}{a}.\frac{qa^4}{D^*}\left(\frac{k_h}{T}\right)\frac{\partial h}{\partial R} \tag{64}$$

The in-plane displacement along y-axis becomes:

$$v = ts.\frac{N}{a\beta}.\frac{qa^4}{D^*}\left(\frac{k_h}{T}\right)\frac{\partial h}{\partial Q} \tag{65}$$

The deflection equation of the plate as:

$$w = (\,Cos2\pi R - 1).(Cos2\pi Q - 1).\frac{qa^4}{D^*}\left(\frac{k_h}{T}\right) \tag{66}$$

The six stress elements are presented in Equations 15 to 20 as:

$$\sigma_x = \frac{\mathrm{E}}{(1+\mu)(1-2\mu)}\left[\,(1-\mu)\,\frac{\mathrm{ts}}{\mathrm{a}}.\frac{\partial^2 h}{\partial R^2} + \mu\frac{\mathrm{ts}}{\mathrm{a}\beta}.\frac{\partial^2 h}{\partial Q^2} + \mu\frac{1}{\mathrm{t}}.\frac{qa^4}{D^*}\left(\frac{k_h}{T}\right)\frac{\partial \mathrm{h}}{\partial \mathrm{S}}\right] \tag{67}$$

$$\sigma_y = \frac{\mathrm{E}}{(1+\mu)(1-2\mu)}\left[\frac{\mu\mathrm{ts}}{a}.\frac{\partial^2 h}{\partial R^2} + \frac{(1-\mu)\mathrm{ts}}{a\beta}.\frac{\partial^2 h}{\partial Q^2} + \frac{\mu}{t}.\frac{qa^4}{D^*}\left(\frac{k_h}{T}\right)\frac{\partial \mathrm{h}}{\partial \mathrm{S}}\right] \tag{68}$$

$$\sigma_z = \frac{\mathrm{E}}{(1+\mu)(1-2\mu)}\left[\frac{\mu\mathrm{ts}}{a}.\frac{\partial^2 h}{\partial R^2} + \frac{\mu\mathrm{ts}}{a\beta}.\frac{\partial^2 h}{\partial Q^2} + \frac{(1-\mu)}{t}.\frac{qa^4}{D^*}\left(\frac{k_h}{T}\right)\frac{\partial \mathrm{h}}{\partial \mathrm{S}}\right] \tag{69}$$

$$\tau_{xy} = \frac{E(1-2\mu)}{(1+\mu)(1-2\mu)}.\left[\frac{\mathrm{ts}}{2a\beta}.\frac{\partial^2 \partial h}{\partial R\,\partial Q} + \frac{\mathrm{ts}}{2a}.\frac{\partial^2 \partial h}{\partial R\,\partial Q}\right] \tag{70}$$

$$\tau_{xz} = \frac{(1-2\mu)E}{(1+\mu)(1-2\mu)}.\left[\frac{1}{2}\frac{\partial \mathrm{h}}{\partial R} + \frac{1}{2a}.\frac{qa^4}{D^*}\left(\frac{k_h}{T}\right)\frac{\partial h}{\partial R}\right] \tag{71}$$

$$\tau_{yz} = \frac{(1-2\mu)E}{(1+\mu)(1-2\mu)}.\left[\frac{1}{2}\frac{\partial \mathrm{h}}{\partial Q} + \frac{1}{2a\beta}.\frac{qa^4}{D^*}\left(\frac{k_h}{T}\right)\frac{\partial h}{\partial Q}\right] \tag{72}$$

Thus, the stiffness coefficients of CCCC rectangular plate is obtained from Equations 34 to 39 and presented in the Table 1.

Table 1. Trigonometric form of stiffness coefficients of CCCC rectangular plate

Deflection form	k_x	k_{xy}	k_y	k_z	k_{2z}	k_h
Trigonometry	$12\pi^4$	$4\pi^4$	$12\pi^4$	$3\pi^2$	$3\pi^2$	1.0

4. Results and Discussion

The parametric data for the trigonometric stiffness coefficient, k_x, k_{xy}, k_y, k_z, k_{2z} and k_q for CCCC shape functions are presented in Table 1. This data was obtained by substituting Equation 58 into Equations 30, 31, 32, 33, 34 and 35 as presented in the Figure 5. This stiffness coefficients were used to obtain the value of the shape functions and displacement and rotation of the plate material when subjected to a uniformly distributed transverse load under the same boundary conditions. The graph in Figure 5 showed that k_x and k_y have the highest coefficient followed by k_{xy} while k_z, k_{2z} and k_q contains the lowest amount of stiffness coefficient.

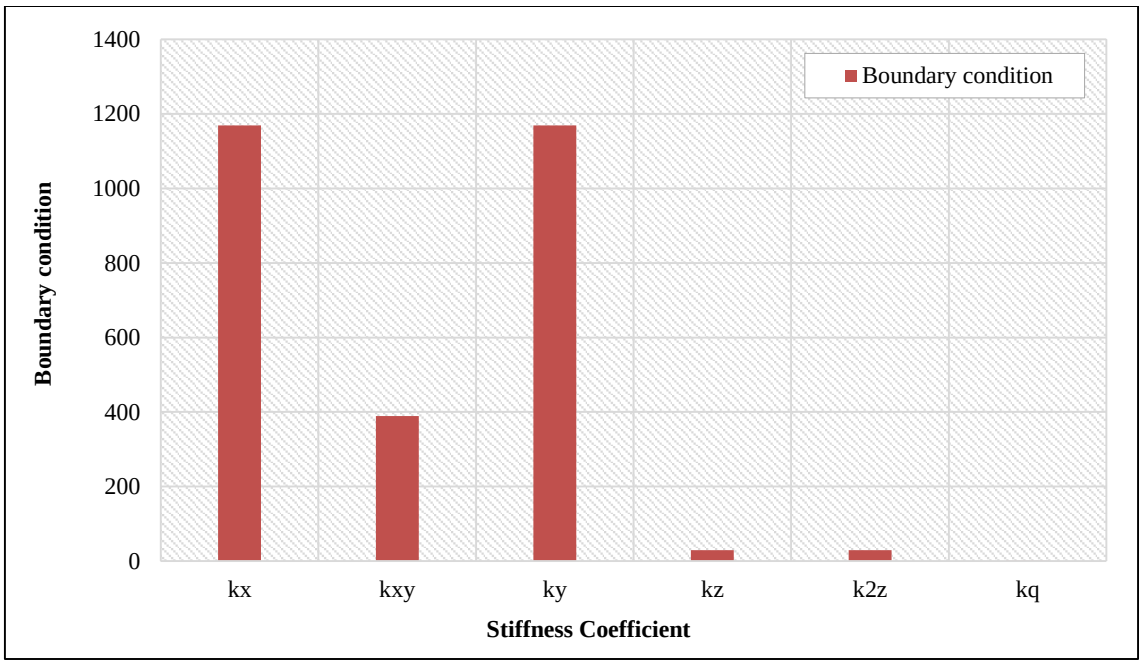

Figure 5. Stiffness coefficient for the CCCC plate boundary condition

The numerical results of the non-dimensional displacements (u, v & w) and the stresses characteristics of a 3-D clamped rectangular plate which was subjected to uniform distributed load was obtained using the established exact trigonometric displacement function. Figures 6 and 7 contains the result of the non-dimensional value of displacements and stresses at different span-thickness aspect ratio in a rectangular thick plate aspect ratio of 1 and 2 respectively.

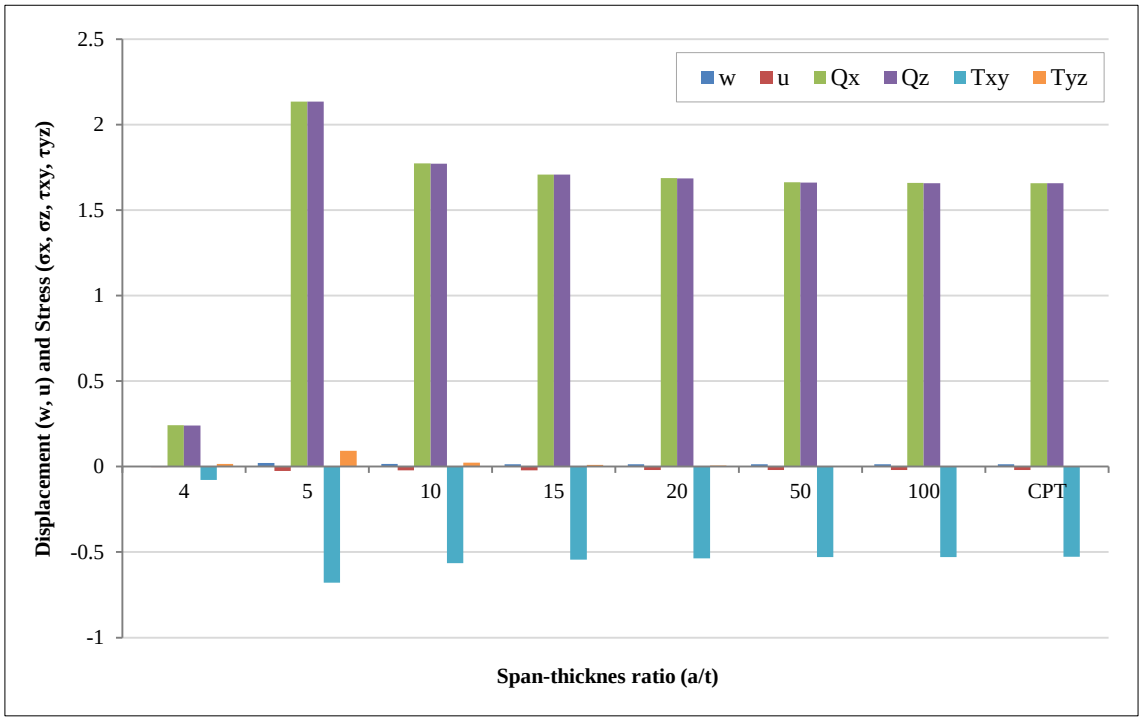

Figure 6. The result of displacements and stresses of a clamped square plates

The result covered the 3-D bending and stress analysis of rectangular plate at varying thickness. The span to thickness ratio considered is ranged between 4, 5, 10, 15, 20, 50, 100 and CPT, which is obviously seen to span from the thick plate, moderately thick plate and thin plate [22]. The present work obtained non-dimensional result of stresses and displacements of the plate by expressing the deflection and rotation functions in the form of trigonometry to analyze the bending characteristics of the plate.

The non-dimensional result in the Figure 6 shows that as the span-thickness ratio of the plate increase, the in-plane displacement along x and y axis (u and v) increases too, whereas, the deflection (w) which occurs at the plate due to the

applied load decrease with increases in the value of the span-thickness ratio of the plate. On the other hand, the stress perpendicular to the x, y and z axis (σ_x, σ_y & σ_z) decreases as the span-depth ratio of the plate increases. Meanwhile, the increase at the span-thickness ratio of the plate increases the value shear stress along the x-y (τ_{xy}) while the span - depth ratio causes a decrease in the value shear stress along the x-z and y-z plane (τ_{xz} & τ_{yz}). These decrease continue until failure occurs in the plate structure.

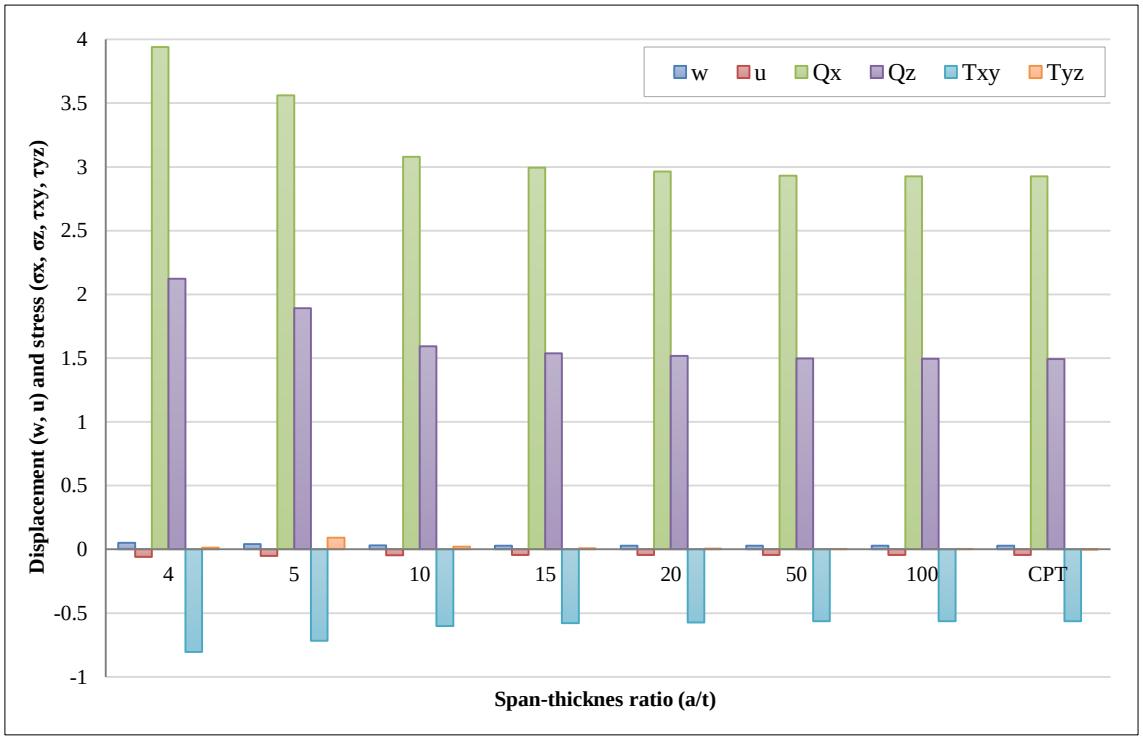

Figure 7, Displacement and stresses of a CCCC plate aspect ratio of 2

Figure 6 shows that, at a span-thickness ratio between 4 and 20, the value of out of plane displacement varies between 0.0026 and 0.0137. These values maintain a constant value of 0.0132 at the span - thickness 50 till 100 which is the same as the CPT. A variation in deflection is discovered more when the plate is thicker and less when the span-thickness increase (thinner plate) under the same loading capacity/condition. This deflection becomes constant and equal to the value of the CPT at span-thickness ratio of 50 and above under the same loading capacity/condition. These decrease continue until the plate structure deflects beyond the elastic yield stress, hence, failure occurs. Thus, it can be said that at span – thickness ratio between 4 and 20 the plate is regarded as thick. The span – thickness ratio beyond 20 till 50 the plate is regarded as moderately thick while the thin plate is regarded as those beyond span – thickness ratio beyond 50.

The non-dimensional result in the Figure 7 shows that as the span-thickness ratio of the plate increase, the in-plane displacement along x and y axis (u and v) increases too, whereas, the deflection (w) which occurs at the plate due to the applied load decrease with increases in the value of the span-thickness ratio of the plate. On the other hand, the stress perpendicular to the x, y and z axis(σ_x, σ_y & σ_z) decreases as the span-depth ratio of the plate increases. Meanwhile, the increase at the span-thickness ratio of the plate increases the value shear stress along the x-y (τ_{xy}) while the span-depth ratio causes a decrease in the value shear stress along the x-z and y-z plane (τ_{xz} & τ_{yz}).

Figure 7 shows that, at a span-thickness ratio between 4 and 20, the value of out of plane displacement varies between 0.0509 and 0.0291. These values maintain a constant value of 0.0283 at the span - thickness 50 till 100 which is equal to the value of the CPT. A variation in deflection is discovered more when the plate is thicker and less when the span-thickness increase (thinner plate) under the same loading capacity/condition. This deflection becomes constant and the same as the CPT at span-thickness ratio of 50 and above under the same loading capacity/condition. These decrease continue until the plate structure deflects beyond the elastic yield stress, hence, failure occurs. Thus, it can be said that at span – thickness ratio between 4 and 20 the plate is regarded as thick. The span – thickness ratio beyond 20 till 50 the plate is regarded as moderately thick while the thin plate is regarded as those beyond span – thickness ratio beyond 50.

Study in the Figure 6 and 7 shows that as the aspect ratio of the plate increase, the in-plane displacement along x and y axis (u and v) decrease whereas, the deflection (w) which occurs at the plate due to the applied load increase with increases in the value of the span-thickness ratio of the plate. On the other hand, the stress perpendicular to the x, y and z axis (σ_x, σ_y & σ_z) increases as the span-depth ratio of the plate increases. This means that, if the plate material is stretched beyond the elastic limit, the failure in a plate structure is bound to occur as the more stresses are induced within

the plate element which affects the performance in terms of the serviceability of the plate. Thus, caution must be taken when selecting the depth and other dimensions along the x and y co-ordinate of the plate to ensure accuracy of the analysis and safety in the construction.

In summary, there are three categories of rectangular plates. The plates whose deflection and vertical shear stress do not vary much with CPT is categorized as thin plate. Hence, the plate whose deflection and transverse shear stress varies very much from zero is categorized as thick plates. Thus, the span-thickness ratio for these categories of rectangular plates are: Thick plate is categorized as the plate with the span to thickness ratio: $a/t \leq 20$ while the thin plate is categorized as the plate with the span-thickness ratio: $a/t \geq 100$. In between the thick and thin plate exist, the moderately thick plate. Thick plate is categorized as the plate with the span-thickness ratio: $a/t > 20 < 50$. Meanwhile, the present theory stress prediction shows that the result of the displacement and stress of thin and moderately thick plate using the 3-D theory is the same for the bending analysis of rectangular plate under the CCCC boundary condition.

The comparative analysis was performed in this study as presented in the Table 2 and Table 3 to show the disparity between different theories used in the plate analysis. This theory includes the analytical process ranging from Double integration, according to Levi, Mindlin theory, FSDT, HSDT and 3-D elasticity. Numerical and approximate approaches were also adopted to compare and show the validity of the derived relationships. The present study was also validated with the past works using different shape or mathematical functions such as polynomial, exponential, hyperbolic and trigonometric displacement functions. The result of the percentage difference evaluation showed that the plate with the largest thickness (a/t of 4) gives a percentage difference of 1.74, 0.55, 0.37, 0.37, 1.29, 1.01 and 3.12% of the work of Ibearugbulem et al. (2018) [28], Ibearugbulem & Onyeka (2020) [34], Li et al. (2015) [35], Liu & Liew (1998) [36], Lok & Cheng (2001) [37], Shen & He (1995) [38] and Zhong & Xu (2017) [39] respectively, when compared with the present study. On the other hand, the thick plate at a/t of 10 gives a percentage difference of 0.33, 0.98, 0.98, 0.98, 1.64, 0.98% and 2.95% of the work of Ibearugbulem et al. (2018) [28], Ibearugbulem & Onyeka (2020) [34], Li et al. (2015) [35], Liu & Liew (1998) [36], Lok & Cheng (2001) [37], Shen & He (1995) [38] and Zhong & Xu (2017) [39] respectively, when compared with the present study. More so, the thick plate at a/t of 20 gives a percentage difference of 0.80, 0.80, 2.85, 2.85 and 2.89% of the work of Ibearugbulem et al. (2018) [28], Ibearugbulem & Onyeka (2020) [34], Li et al. (2015) [35], Liu & Liew (1998) [36] and Shen & He (1995) [38] respectively, when compared with the present study. The result of the work of Lok & Cheng (2001) [37] and Zhong & Xu (2017) [39] at a/t of 20 is not available in the literature in consideration. Table 3 shows that, the difference with past works in consideration percentagewise decreases and converges as the plate is getting thinner. It can be deduced that, the difference with past works in consideration percentagewise at a/t of 10 and 20 gives a constant value of 0.15% and 0.13% respectively, a value which could be the same difference when compared with the value of the CPT.

Table 2. Comparative deflection analysis for square plate at varying span-thickness ratio (β = a/t) between present study and past studies

a/t	Present	[28]	[34]	[35]	[36]	[37]	[38]	[39]
5	0.2178	0.214	0.219	0.217	0.217	0.215	0.220	0.211
10	0.1525	0.153	0.154	0.151	0.151	0.150	0.151	0.148
20	0.1369	0.138	0.138	0.133	0.133	-	0.133	-

From Table 3, it is found that the average the difference with 3-D elasticity trigonometric theory percentagewise and those of the 2-D HSDT with assumed polynomial shape function [30] and 2-HSDT with exact shape function [34] is 0.36% and 0.29% respectively. The average the difference percentagewise with 2-D Mindlin FSDT [37, 39] is about 2.41% and 3.62%, while the average difference percentagewise with the 2-D thick plate numeric analysis [35] and moderately thick [38] is 53% and 61% respectively.

Table 3. Percentage difference between the present study and past studies

	$\%\mathbf{Diff} = \frac{\textbf{Absolute difference betwee present and pasr value}}{\textbf{Past value}}$						
Span-to depth ratio (a/t)	[28]	[34]	[35]	[36]	[37]	[38]	[39]
5	1.745	0.551	0.367	0.367	1.286	1.010	3.122
10	0.328	0.984	0.984	0.984	1.639	0.984	2.951
20	0.804	0.804	2.849	2.849	-	2.849	-
Average % Difference	0.36	0.29	0.53	0.52	2.41	0.61	3.62
Total Ave.% Difference				1.19			

The overall average difference percentage wise with 2-D Mindlin FSDT [37, 39] is about 3.02% while the overall average difference percentagewise with the 2-D numeric analysis [36, 39] is about 0.62%. The present study overall average difference values of deflection percentagewise with those using 2-D HSDT shape functions [30, 34] is about 0.33%. This negligible difference showed that HSDT is preferable to the Levi, Mindlin theory and numerical method in the thick plate analysis. Consequently, the smaller value of percentage between the present study and those of 2-D HSDT (0.33%) showed that HSDT using derived polynomial displacement function is better compared to those of HSDT with an assumed shape function as it predicted an exact deflection which proved more reliable in the analysis of thick plate under the same boundary condition. Despite the fact that both Ibearugbulem et al. (2018) [28], Ibearugbulem & Onyeka (2020) [34], Li et al. (2015) [35], Liu & Liew (1998) [36], Lok & Cheng (2001) [37], Shen & He (1995) [38] and Zhong & Xu (2017) [39] used shear deformation theory their work differs more when compared with the present study. This shows that HSDT derived shape function, enhanced close form solution in plate analysis. However, the overall average difference values of deflection percentagewise with Ibearugbulem et al. (2018) [28], Ibearugbulem & Onyeka (2020) [34], Li et al. (2015) [35], Liu & Liew (1998) [36], Lok & Cheng (2001) [37], Shen & He (1995) [38] and Zhong & Xu (2017) [39] is 1. 19%. This showed that at the 98 % confidence level, both theory and methods are the same for a thick plate analysis.

It is worth noting that the 2-D RPT with exact deflection gives a closer result when compared with exact 3-D plate theory than those 2-D RPTs with an assumed deflection and other RPT and CPT in the thick plate analysis. Hence, an exact 3-D theory is required to achieve efficiency. Thus, the present model uses the six stress elements to yield the exact solution for the analysis of a thick plate that is clamped and supported on all the edges (CCCC). Hence, the result of the present analysis, which contains all the stress elements with an exact deflection function, ensures that the variation of the stresses through the thickness of the plate which induces stresses can be used with confidence for bending analysis of the plate.

5. Conclusions

The 3-D bending and stress analysis of thick rectangular plates using 3-D elasticity theory has been investigated, and the following conclusion has been drawn:

- A closer-form solution is predicted by the trigonometric shape function than by the polynomial displacement function.
- The present theory of stress prediction shows that the result of the displacement and stress of thin and moderately thick plates using the 3-D theory is the same at a span-thickness ratio beyond 50% for the bending analysis of rectangular plates under the CCCC boundary condition.
- Classical theory is good for thin plates but over-predicts buckling loads in relatively thick plates.
- Plate analysis requires 3-D analogy for a true solution, but the 2-D shear deformation theory gives an approximate solution which is practically unrealistic.
- The 3-D exact plate model developed in this study can be used in the analysis of any category of the plate.

6. Declarations

6.1. Author Contributions

Conceptualization, F.C.O., T.E.O. and B.O.M.; methodology, F.C.O., T.E.O. and B.O.M.; software, F.C.O., T.E.O. and B.O.M.; formal analysis, F.C.O., T.E.O. and B.O.M.; writing—original draft preparation, F.C.O., T.E.O. and B.O.M.; writing—review and editing, F.C.O., T.E.O. and B.O.M. All authors have read and agreed to the published version of the manuscript.

6.2. Data Availability Statement

Data sharing is not applicable to this article.

6.3. Funding

The authors received no financial support for the research, authorship, and/or publication of this article.

6.4. Ethical Approval

Not applicable.

6.5. Declaration of Competing Interest

The authors declare that they have no known competing financial interests or personal relationships that could have appeared to influence the work reported in this paper.

7. References

[1] Chandrashekhara, K. (2001). Theory of plates. University Press, Hyderabad, India.

[2] Onyeka, F. C., Okafor, F. O., & Onah, H. N. (2019). Application of exact solution approach in the analysis of thick rectangular plate. International Journal of Applied Engineering Research, 14(8), 2043-2057.

[3] Mahi, A., Adda Bedia, E. A., & Tounsi, A. (2015). A new hyperbolic shear deformation theory for bending and free vibration analysis of isotropic, functionally graded, sandwich and laminated composite plates. Applied Mathematical Modelling, 39(9), 2489–2508. doi:10.1016/j.apm.2014.10.045.

[4] Timoshenko, S., & Woinowsky-Krieger, S. (1959). Theory of plates and shells (2nd Ed.). McGraw-hill, New York City, United States.

[5] Chukwudi, O. F., Edozie, O. T., & Chidobere, N.-D. (2022). Buckling Analysis of a Three-Dimensional Rectangular Plates Material Based on Exact Trigonometric Plate Theory. Journal of Engineering Research and Sciences, 1(3), 106–115. doi:10.55708/js0103011.

[6] Onyeka, F. C., Mama, B. O., & Okeke, T. E. (2022). Exact Three-Dimensional Stability Analysis of Plate Using a Direct Variational Energy Method. Civil Engineering Journal (Iran), 8(1), 60–80. doi:10.28991/CEJ-2022-08-01-05.

[7] Onyeka, F. C., & Mama, B. O. (2021). Analytical study of bending characteristics of an elastic rectangular plate using direct variational energy approach with trigonometric function. Emerging Science Journal, 5(6), 916–928. doi:10.28991/esj-2021-01320.

[8] Reddy, J. N. (2006). Theory and analysis of elastic plates and shells (2nd Ed.). CRC Press, Boca Raton, United States. doi:10.1201/9780849384165.

[9] Ghugal, Y. M., & Gajbhiye, P. D. (2016). Bending analysis of thick isotropic plates by using 5th order shear deformation theory. Journal of Applied and Computational Mechanics, 2(2), 80–95. doi:10.22055/jacm.2016.12366.

[10] Shimpi, R. P., & Patel, H. G. (2006). A two variable refined plate theory for orthotropic plate analysis. International Journal of Solids and Structures, 43(22–23), 6783–6799. doi:10.1016/j.ijsolstr.2006.02.007.

[11] Gujar, P. S., & Ladhane, K. B. (2015). Bending analysis of simply supported and clamped circular plate. International Journal of Civil Engineering, 2(5), 45-51. doi:10.14445/23488352/ijce-v2i5p112.

[12] Sadrnejad, S. A., Daryan, A. S., & Ziaei, M. (2009). Vibration equations of thick rectangular plates using Mindlin plate theory. Journal of Computer Science, 5(11), 838–842. doi:10.3844/jcssp.2009.838.842.

[13] Szilard, R. (2004). Theories and Applications of Plate Analysis: Classical Numerical and Engineering Methods. John Wiley & Sons, Hoboken, United States. doi:10.1002/9780470172872.

[14] Kwak, S., Kim, K., Jon, S., Yun, J., & Pak, C. (2022). Free vibration analysis of laminated rectangular plates with varying thickness using Legendre-radial point interpolation method. Computers & Mathematics with Applications, 117, 187-205. doi:10.1016/j.camwa.2022.04.020.

[15] Song, Y., Xue, K., & Li, Q. (2022). A solution method for free vibration of intact and cracked polygonal thin plates using the Ritz method and Jacobi polynomials. Journal of Sound and Vibration, 519, 116578. doi:10.1016/j.jsv.2021.116578.

[16] Sadrnejad, S. A., Daryan, A. S., & Ziaei, M. (2009). Vibration equations of thick rectangular plates using Mindlin plate theory. Journal of Computer Science, 5(11), 838–842. doi:10.3844/jcssp.2009.838.842.

[17] Ibearugbulem, O. M. (2013). Pure bending analysis of thin rectangular SSSS plate Using Taylor-Mclaurin series. International Journal of Civil and Structural Engineering, 3(4), 685–691. doi:10.6088/ijcser.201203013062.

[18] Reissner, E. (1945). The Effect of Transverse Shear Deformation on the Bending of Elastic Plates. Journal of Applied Mechanics, 12(2), A69–A77. doi:10.1115/1.4009435.

[19] Hashemi, S. H., & Arsanjani, M. (2005). Exact characteristic equations for some of classical boundary conditions of vibrating moderately thick rectangular plates. International Journal of Solids and Structures, 42(3–4), 819–853. doi:10.1016/j.ijsolstr.2004.06.063.

[20] Reissner, E. (1981). A note on bending of plates including the effects of transverse shearing and normal strains. ZAMP Zeitschrift Für Angewandte Mathematik Und Physik, 32(6), 764–767. doi:10.1007/BF00946987.

[21] Reddy, J. N. (1984). A refined nonlinear theory of plates with transverse shear deformation. International Journal of Solids and Structures, 20(9–10), 881–896. doi:10.1016/0020-7683(84)90056-8.

[22] Obst, M., Wasilewicz, P., & Adamiec, J. (2022). Experimental investigation of four-point bending of thin walled open section steel beam loaded and set in the shear center. Scientific Reports, 12(1), 1-17. doi:10.1038/s41598-022-10035-z.

[23] Sayyad, A. S., & Ghugal, Y. M. (2012). Bending and free vibration analysis of thick isotropic plates by using exponential shear deformation theory. Applied and Computational Mechanics, 6(1), 65-82.

[24] Onyechere, Ignatius Chigozie, Ibearugbulem, O. M., Collins Anya, U., Okechukwu Njoku, K., Igbojiaku, A. U., & Gwarah, L. S. (2020). The Use of Polynomial Deflection Function in The Analysis of Thick Plates using Higher Order Shear Deformation Theory. Saudi Journal of Civil Engineering, 4(4), 38–46. doi:10.36348/sjce.2020.v04i04.001.

[25] Selvaraj, R., Maneengam, A., & Sathiyamoorthy, M. (2022). Characterization of mechanical and dynamic properties of natural fiber reinforced laminated composite multiple-core sandwich plates. Composite Structures, 284, 115141. doi:10.1016/j.compstruct.2021.115141.

[26] Nwoji, C. U., Onah, H. N., Mama, B. O., & Ike, C. C. (2018). Ritz variational method for bending of rectangular Kirchhoff plate under transverse hydrostatic load distribution. Mathematical Modelling of Engineering Problems, 5(1), 1–10. doi:10.18280/mmep.050101.

[27] Ike, C. C. (2017). Kantorovich-Euler Lagrange-Galerkin's method for bending analysis of thin plates. Nigerian Journal of Technology, 36(2), 351. doi:10.4314/njt.v36i2.5.

[28] Ibearugbulem, O. M., Ezeh, J. C., Ettu, L. O., & Gwarah, L. S. (2018). Bending analysis of rectangular thick plate using polynomial shear deformation theory. IOSR Journal of Engineering (IOSRJEN), 8(9), 53-61.

[29] Festus, O., & Okeke, E. T. (2021). Analytical Solution of Thick Rectangular Plate with Clamped and Free Support Boundary Condition using Polynomial Shear Deformation Theory. Advances in Science, Technology and Engineering Systems Journal, 6(1), 1427–1439. doi:10.25046/aj0601162.

[30] Festus, O., Okeke, E. T., & John, W. (2020). Strain–Displacement expressions and their effect on the deflection and strength of plate. Advances in Science, Technology and Engineering Systems, 5(5), 401–413. doi:10.25046/AJ050551.

[31] Grigorenko, A. Y., Bergulev, A. S., & Yaremchenko, S. N. (2013). Numerical Solution of Bending Problems for Rectangular Plates. International Applied Mechanics, 49(1), 81–94. doi:10.1007/s10778-013-0554-1.

[32] Onyeka, F. C. & Ibearugbulem, O. M. (2020). Load Analysis and Bending Solutions of Rectangular Thick Plate. International Journal on Emerging Technologies, 11(3): 1103–1110.

[33] Fu, G., Tuo, Y., Sun, B., Shi, C., & Su, J. (2022). Bending of variable thickness rectangular thin plates resting on a double-parameter foundation: integral transform solution. Engineering Computations, 39(7), 2689-2704. doi:10.1108/EC-11-2021-0692.

[34] Ibearugbulem, O. M., & Onyeka, F. C. (2020). Moment and Stress Analysis Solutions of Clamped Rectangular Thick Plate. European Journal of Engineering Research and Science, 5(4), 531–534. doi:10.24018/ejers.2020.5.4.1898.

[35] Li, R., Ni, X., & Cheng, G. (2015). Symplectic Superposition Method for Benchmark Flexure Solutions for Rectangular Thick Plates. Journal of Engineering Mechanics, 141(2), 1–17. doi:10.1061/(asce)em.1943-7889.0000840.

[36] Liu, F. L., & Liew, K. M. (1998). Differential cubature method for static solutions of arbitrarily shaped thick plates. International Journal of Solids and Structures, 35(28–29), 3655–3674. doi:10.1016/S0020-7683(97)00215-1.

[37] Lok, T. S., & Cheng, Q. H. (2001). Bending and forced vibration response of a clamped orthotropic thick plate and sandwich panel. Journal of Sound and Vibration, 245(1), 63–78. doi:10.1006/jsvi.2000.3543.

[38] Shen, P., & He, P. (1995). Bending analysis of rectangular moderately thick plates using spline finite element method. Computers & Structures, 54(6), 1023-1029. doi:10.1016/0045-7949(94)00401-N.

[39] Zhong, Y., & Xu, Q. (2017). Analysis Bending Solutions of Clamped Rectangular Thick Plate. Mathematical Problems in Engineering, 2017, 1–6. doi:10.1155/2017/7539276.